TITLE PAGE

Piperine is a Mechanism-based inactivator of CYP3A

Tiantian Cui, Qian Wang, Xiaoxiao Tian, Kehan Zhang,
Ying Peng*, and Jiang Zheng*

State Key Laboratory of Functions and Applications of Medicinal Plants (J.Z.), Key Laboratory of Pharmaceutics of Guizhou Province and Guizhou Medical University, Guiyang, Guizhou 550004, P. R. China; Key Laboratory of Environmental Pollution Monitoring and Disease Control (J.Z.), Ministry of Education, Guizhou Medical University, Guiyang, 550025, P. R. China; Wuya College of Innovation (T.C., Q.W., X.T., K.Z., Y.P., J.Z.), Shenyang Pharmaceutical University, Shenyang, Liaoning 110016, P. R. China School of Pharmacy.

RUNNING TITLE PAGE

Running Title: Inactivation of CYP3A by piperine

Corresponding Authors:
Jiang Zheng, PhD
State Key Laboratory of Functions and Applications of Medicinal Plants, Key Laboratory of Pharmaceutics of Guizhou Province, Guizhou Medical University, Guiyang, Guizhou, 550004, P. R. China; Wuya College of Innovation, Shenyang Pharmaceutical University, Shenyang, P. R. China;
E-mail: zhengneu@yahoo.com
Tel: +86-24-23984215
Fax: +86-24-23986510

The two corresponding units contributed equally to this work.

Ying Peng, PhD
Wuya College of Innovation, Shenyang Pharmaceutical University, Shenyang, Liaoning, 110016, P. R. China
E-mail: yingpeng1999@163.com
Tel: +86-24-23986361
Fax: +86-24-23986510

The number of text pages: 52
The number of figures: 11
The number of references: 42
The number of words in the *Abstract*: 175
The number of words in the *Introduction*: 691
The number of words in the *Discussion*: 970

Abbreviations: PPR, piperine; DM-PPR, demethylene piperine; MBI(s), mechanism-based inactivator(s); MIC, metabolic-intermediate complex; MDP, methylenedioxyphenyl; IS, internal standard; CYPs, cytochrome P450 enzymes; HLMs, human liver microsomes; DDQ, 2,3-dichloro-5,6-dicyano-1,4-benzoquinone; LC-MS/MS, liquid chromatography coupled to tandem mass spectrometry; MRM, multiple reaction monitoring; EPI, enhanced product ion; NADPH, β-nicotinamide adenine dinucleotide 2'-phosphate reduced tetrasodium salt; GSH, glutathione; ROS, reactive oxygen species; SOD, superoxide dismutase; NAC, N-acetylcysteine; PBS, potassium phosphate buffer.

Abstract

Piperine (PPR) is the representative alkaloid component of piper species (family: Piperaceae). Our rapid screening study found PPR caused time-dependent inhibition of cytochrome P450s (CYP) 3A and 2D6, and CYP3A was inactivated the most. Further study demonstrated PPR is a time-, concentration-, and NADPH-dependent inhibitor of CYP3A, and significant loss (49.5 ± 3.9%) of CYP3A activity was observed after 20 min incubations with 80 μM PPR at 37 °C. The values of K_I and k_{inact} were 30.7 μM and 0.041 min^{-1}, respectively. CYP3A competitive inhibitor ketoconazole showed protective effect against the enzyme inactivation. Superoxide dismutase/catalase and GSH displayed minor protection against the PPR caused enzyme inactivation. Ferricyanide partially reduced the enzyme inhibition by PPR. Additionally, NADPH-dependent formation of reactive metabolites from PPR were found in human liver microsomal incubation mixtures. An *ortho*-quinone intermediate was trapped by NAC in microsomal incubations with PPR. DM-PPR, demethylene metabolite of PPR, showed weak enzyme inactivation relative to that caused by PPR. It appears that both carbene and *ortho*-quinone intermediates were involved in the inactivation of CYP3A caused by PPR.

Significance Statement

CYP3A subfamily members (mainly CYP3A4 and CYP3A5) play a critical role in drug metabolism. Piperine (PPR), a methylenedioxyphenyl derivative combined with an unsaturated ketone, is the major active ingredient of pepper. PPR revealed time- and concentration-, and NADPH-dependent inhibitory effect on CYP3A. Carbene and quinone metabolites were both involved in the observed CYP3A inactivation by PPR. Apparently, the unsaturated ketone moiety did not participate in the enzyme inactivation. The present study sounds an alert of potential risk for food-drug interactions.

Introduction

Piperis fructus, near-maturely or maturely dried fruits of *Piper nigrum*, are commonly used as dietary spices, such as food additives and condiments (Wattanathorn et al., 2008). Piperine (1-piperoylpiperidine, PPR) is a dominant alkaloid occurring in the fruits of long pepper (*Piper longum* Linn), black pepper (*Piper nigrum* Linn), and other piper species (family: Piperaceae) (Wattanathorn et al., 2008; Gupta et al., 2015; Umar et al., 2013). In addition, pepper has had a long history of medicinal use in Asian and Pacific islands (Umar et al., 2013; Bae et al., 2010). It is also often employed to treat diseases related to the gastrointestinal tract, particularly in Ayurvedic medicines (Gupta et al., 2015; Johri et al., 1992). PPR was reported to possess multiple excellent and extensive pharmacological effects, such as anti-inflammatory (Bang et al., 2009; Murunikkara et al., 2012; Tasleem et al., 2014), analgesic (Tasleem et al., 2014), antioxidant (Zarai et al., 2013; Chonpathompikunlert et al., 2010; Samra et al., 2016), bioavailability enhancer (Katiyar et al., 2016), and anticonvulsant effect (Bukhari et al., 2013). Additionally, PPR reportedly attenuated collagenase-mediated tendon injury (Gong et al., 2017). The structure of PPR can be divided into three parts: heteroaromatic ring, aliphatic chain, and piperidine ring. A number of PPR derivatives with modified piperine have been reported to show pharmacologic properties, including inhibition of NorA efflux pump (Kumar et al., 2008), anticancer, and antibacterial activity (Rama Subba Rao et al., 2012; Umadevi et al., 2013).

P450 (CYP) enzymes are the major enzymatic system responsible for elimination many pharmaceutical agents (Lee et al., 2012). Inhibition of CYP enzymes may result

in serious consequences, particularly for the medicinal agents with narrow therapeutic window (VandenBrink et al., 2010; Parkinson et al., 2011). The inhibition of CYP enzymes can be roughly divided into two types: direct inhibition by parent compounds and metabolism-dependent inhibition (MDI) by metabolites (Lee et al., 2012). MDI includes reversible, quasi-irreversible, and irreversible inhibition (Lin et al., 1998). The latter two are classified as mechanism-based inhibition (MBI). Methylenedioxyphenyl (MDP) compounds are an important class of chemicals widely occurring in insecticides, oils, and spices (Murray, 2000). As early as 1970, MDP compounds were found to enhance the toxicity of insecticides, which was reportedly achieved by inhibiting the mixed-function oxidase system of microsomes (Casida et al., 1970). Many compounds containing such structure are microsomal substrates as well as inhibitors and have been documented to cause CYP inactivation. Alkaloids canadine, bulbocanine, and carnitine were reported to be mechanism-based and quasi-irreversible inactivators of CYP2C19 (Salminen et al., 2011). Myristicin is a mechanism-based inactivator of CYP1A2, and the reactive metabolites involved in the enzyme inactivation are quinone tautomers (Yang et al., 2015). Five kinds of MDP lignans found in piper cubeba were documented to be irreversible inhibitors of CYP3A4 reportedly resulting from their metabolic activation (Usia et al., 2005). Two reactive metabolites/intermediates derived from MDP-containing compounds are suggested to be responsible for the host enzyme inactivation, including catechol metabolites and carbene intermediates. The carbene intermediates can coordinate with the heme of CYP enzymes. The formation of carbene-heme-iron-porphyrin complexes results in

quasi-irreversible inhibition of CYPs (Taxak et al., 2013). The catechols can be further oxidized to reactive *ortho*-quinones which sequentially alkylate apoprotein of CYPs (Hutzler et al., 2006; 2008).

Intake of foods may induce the expression or inhibit the activity of CYP enzymes, which may interfere the pharmacokinetic properties of various drugs. For instance, grapefruits juice ingestion can specifically inhibit CYP3A4-mediated drug metabolism (Ohnishi et al., 2010). Furanocoumarin epoxybergamottin, a component squeezed from the peel of grapefruits into the juice during industrial manufacturing, was found to demonstrate inhibitory activity on CYP3A (Wangensteen et al., 2003). CYP3A is the major P450 subfamily extensively distributed in hepatocytes and intestine epithelial cells (Rendic et al., 1997; Murray et al., 2012).

In this paper, we studied the inhibitory effect of PPR on human hepatic CYP enzymes and characterized the reactive metabolites possibly involved in the enzyme inactivation. The significance of the present study is to understand the biochemical mechanism of the interaction of CYP enzymes with PPR, which is important to the justification of potential food-drug interactions resulting from PPR to ensure the safety and effectiveness of medications.

Materials and Methods

Chemicals. Piperine (PPR) with purity > 98% was acquired from Dalian Meilun Biotechnology Co., Ltd. (Dalian, China). Superoxide dismutase (SOD) was purchased from Shanghai Jianglai Biologic Technology Co., Ltd. (Shanghai, China). Propranolol, bupropion·HCl, dextromethorphan, tolbutamide, coumarin, testosterone, 4-nitrophenol, phenacetin, *α*-naphthoflavone, pilocarpine, methoxsalen, sulfaphenazole, ticlopidine, quinidine, disulfiram, ketoconazole, NADPH, glutathione (GSH), *N*-acetylcysteine (NAC), and 2,3-dichloro-5,6-dicyano-1,4-benzoquinone (DDQ) were obtained from Sigma-Aldrich (St. Louis, MO). Mixed human liver microsomes prepared from adult male donors and recombinant human CYP enzymes were provided by BD Gentest (Woburn, MA). All organic solvents and reagents were analytical or HPLC grade and purchased from Fisher Scientific (Springfield, NJ). DMSO-d_6 was purchased from CIL (Cambridge Isotope Laboratories, Inc, USA).

Chemical Synthesis of DM-PPR. PPR (4.0 mg) and 8.0 mg of anhydrous $AlCl_3$ were placed in a 25 mL round bottom flask and mixed with 3.0 mL of toluene. The mixture was then refluxed at 110 °C for 12 h, followed by incorporation of additional anhydrous $AlCl_3$ (2.0 mg) and another 12 h refluxing. The resulting mixture was mixed with 0.5 mL of water after cooled to the room temperature, and shaken well. The resulting mixture was concentrated under vacuum. The residue was submitted to a semipreparative liquid chromatography for purification, and purified DM-PPR (Scheme 1) was characterized by MS on Bruker hybrid quadrupole-time-of-flight (Q-TOF) mass spectrometer and NMR on a BRUKER-ARX-600 spectrometer.

Chemical Synthesis of NAC Conjugates. NAC conjugates M1 and M2 were synthesized as follows: PPR (200 μM) was directly mixed with NAC (20 mM) in PBS (100 mM, 2 mL), followed by stirring at 37 °C for 60 min and centrifugation at 19,000 *g*. The supernatants were analyzed by LC-MS/MS. For the synthesis of NAC conjugates M3-M8, DM-PPR (1.0 mg, 3.7 μmol) was dissolved in 2.0 mL of CH_2Cl_2. After mixed with DDQ (2.0 mg, 8.8 μmol), the solution was stirred at 4 °C for 4 h. The organic solvent was removed by evaporation, and the resulting crude products were redissolved in 2.0 mL of water. The mixture was further reacted with NAC (4.0 mg, 25 μmol) with stirring at room temperature for 12 h. The final mixture was centrifuged, and the supernatants (5.0 μL) were subjected to LC-MS/MS for analysis.

Screening of Time-Dependent CYP Inhibition by PPR. Time-course inhibitory effects of PRR on CYPs were determined by monitoring individual CYP activities of human liver microsomes at various time points after being exposed to PPR. The primary incubation mixtures contained PPR (0 or 80 μM), $MgCl_2$ (3.2 mM), and human liver microsomes (0.5 mg protein/mL) in 200 μL PBS (100 mM, pH=7.4). After preincubation at 37 °C for 3 min, NADPH (1.0 mM) was added to the primary incubations to initiate the reactions. After the primary mixtures were incubated for 0, 5, 10, and 20 min, 40 μL aliquots were transferred to the secondary reaction mixtures (120 μL) composed of individual probe substrates (100 μM bupropion for CYP2B6, 50 μM phenacetin for CYP1A2, 5.0 μM dextromethorphan for CYP2D6, 120 μM tolbutamide for CYP2C9, 200 μM 4-nitrophenol for CYP2E1, 200 μM coumarin for CYP2A6, or 200 μM testosterone for CYP3A), $MgCl_2$ (3.2 mM), and NADPH (1.0

mM), and further incubation for 15 min, respectively. Ice-cold acetonitrile (120 μL) containing internal standard (IS) propranolol (100 ng/mL) was mixed with the incubation solution to quench the reactions. The resulting supernatants after vortex-mixing and centrifuging were analyzed by LC-MS/MS. The loss of enzyme activities was determined by monitoring the generation of the metabolites resulting from the probe substrates applied in the secondary incubations.

Determination of Time-, Concentration-, and NADPH-Dependent Inhibition of CYP3A. The primary incubation mixtures (200 μL) were composed of PPR at concentrations of 0, 5.0, 10, 20, 40, 60, or 80 μM, $MgCl_2$ (3.2 mM), human liver microsomes (0.5 mg protein/mL) in PBS (100 mM, pH 7.4). After 3 min pre-incubation, the reaction was initiated by addition of NADPH (1.0 mM). At time points of 0, 5, 10, and 20 min, 40 μL of the primary incubations was withdrawn for CYP3A activity assessment in the secondary incubations that contain testosterone (200 μM) and NADPH (1.0 mM) in PBS (100 mM, pH 7.4). After 15 min incubation, the reactions were quenched using ice-cold acetonitrile (120 μL) containing propranolol (100 ng/mL) as IS. The supernatants were analyzed by LC-MS/MS after being centrifuged at 19,000 *g* for 10 min. To determine NADPH-dependence of the observed CYP3A enzyme inhibition, PBS which replaced NADPH with the same volume was included in microsomal incubations with PPR (80 μM).

Determination of Time- and NADPH-Dependent Inhibition of CYP3A by DM-PPR. The inhibitory effect of DM-PPR on CYP3A was evaluated, and similar protocol

as above was executed except for the replacement of PPR with DM-PPR (80 μM). Control incubations lacked DM-PPR or NADPH.

Determination of Effect of Ketoconazole on PPR-Mediated Inactivation of CYP3A. Ketoconazole is a competitive inhibitor of CYP3A. The primary incubation system contained PPR (80 μM), $MgCl_2$ (3.2 mM), human liver microsomes (0.5 mg protein/mL), and ketoconazole at concentrations of 0, 0.01, 0.1, and 1.0 μM. The procedures of subsequent reaction initiation/termination and sample preparation were the same as described above.

Determination of Effects of SOD/Catalase and GSH on PPR-Mediated Inactivation of CYP3A. Nucleophile glutathione (GSH, 2.0 mM) was included in the primary mixture together with PPR (80 μM), $MgCl_2$ (3.2 mM), human liver microsomes (0.5 mg protein/mL), and NADPH (1.0 mM). At 0 and 20 min, the resulting incubation mixtures (40 μL for each) were transferred to the secondary incubations containing probe substrate testosterone for the evaluation of the remaining enzyme activities. In a separate study, similar incubations were performed except incorporation of superoxide dismutase (SOD) and catalase (800 unit/mL for each) to replace GSH. The control groups lacked either GSH or SOD/catalase.

Determination of Partition Ratio. To determine the partition ratio, PPR at final concentrations of 0, 2.0, 5.0, 10, 20, 40, 60, 80, and 100 μM and human recombinant CYP3A4 (50 nM) were mixed in the primary reactions. NADPH (1.0 mM) was added to initiate the reactions. Aliquots (40 μL) were taken at time points of 0 and 20 min

to the secondary incubation mixtures containing testosterone as a probe substrate for measuring the remaining CYP3A4 activities.

Determination of Reversibility of PPR-Mediated CYP3A Inhibition through Dialysis. A mixture of PPR (0 or 80 μM), human liver microsomes (0.5 mg protein/mL), and NADPH (1.0 mM) was incubated at 37 °C for 0 and 20 min. The resulting mixture was transferred into Slide-A-Lyzer cassettes (molecular mass cut off: 3,500 Da, Pierce, Rockford, IL) and dialyzed in 900 mL of PBS (100 mM, pH 7.4) at 4 °C three times for 2 h each time. In parallel, non-dialyzed samples were allowed to stand at 4 °C for 6 h. Aliquots (40 μL) of all samples were submitted to the secondary incubations (120 μL) composed of testosterone as a probe substrate after being brought to room temperature, respectively. CYP3A enzyme activities of the resulting mixtures were determined as stated below.

Determination of Reversibility of PPR-Mediated CYP3A Inhibition by Potassium Ferricyanide. Whether carbene intermediate was involved in PPR-mediated CYP3A inhibition was determined by following reported methods (Watanabe et al., 2007; Hong et al., 2015). Briefly, the primary incubations containing PPR (0 or 80 μM), human liver microsomes (0.5 mg/mL) and NADPH were executed at 37 °C. After 0 or 20 min incubation, the resulting solutions (40 μL) were mixed with $K_3Fe(CN)_6$ (0 or 2.0 mM) dissolved in10 μL of PBS (100 mM, pH 7.4). After 10 min incubation, the mixtures were subjected to the secondary incubation for assessment of the remaining CYP3A activities as below.

P450 Enzyme Assays. The amounts of the products formed from individual probe substrates were measured to evaluate the corresponding CYP enzyme activities by an AB Sciex 5500 triple quadrupole mass spectrometer (Applied Biosystems, Foster City, CA) equipped with an Agilent 1260 Series Rapid Resolution HPLC (Agilent Technologies, Santa Clara, CA). A Promosil C_{18} column (150 × 4.6 mm, 5 μm, Agela Technologies, Inc., Tianjin, China) was employed for analyte separation. The solvent system was composed of mobile phase A (water containing 0.1% formic acid) and phase B (acetonitrile with 0.1% formic acid). The flow rate was maintained at 0.8 mL/min. The gradient elution was set as follows: 1) 0-2.0 min, 90% A; 2.0-2.5 min, 90-70% A; 2.5-14.0 min, 70-30% A; 14.0-14.1 min, 30-10% A; 14.1-15.0 min, 10-90% A; 15.0-17.0 min, 90% A for the products of CYPs2B6, 2D6, and 1A2; 2) 0-2.0 min, 90% A; 2.0-5.0 min, 90-30% A; 5.0-10.0 min, 30-5% A; 10.0-12.0 min, 5% A; 12.0-13.0 min, 5-90% A; 13.0-15.0 min, 90% A for the products of CYPs2C9, 2E1, and 2A6; and 3) 0-3.0 min, 70% A; 3.0-8.0 min, 70-66% A; 8.0-10.0 min, 66-10% A; 10.0-11.0 min, 10% A; 11.0-11.1 min, 10-70% A; 11.1-13.0 min, 70% A for the product of CYP3A. Multiple reaction monitoring (MRM) scan mode was applied to quantitate the products. Ion pairs of MRM acquired included: 152.1→110.0 for acetaminophen (CYP1A2), 256.0 → 238.0 for hydroxybupropion (CYP2B6), 287.2 → 171.2 for 4-hydroxytolbutamide (CYP2C9), 258.2→157.1 for dextrorphan (CYP2D6), 305.3→269.4 for 6β-hydroxytestosterone (CYP3A), and 260.3→116.3 for propranolol (IS) in positive mode, 161.0→105.1 for 7-hydroxycoumarin (CYP2A6) and 153.9→122.8 for 4-nitrocatechol (CYP2E1) in negative mode.

Metabolite Identification. PPR (100 μM), human liver microsomes (1.0 mg protein/mL), $MgCl_2$ (3.2 mM), NAC (10 mM), and NADPH (1.0 mM) were mixed in 100 μL PBS (100 mM, pH 7.4) and incubated at 37 °C for 30 min. NADPH was not included in negative control. The resulting reactions were processed as above, followed by LC-MS/MS analysis. The mobile phase system included water (A) and acetonitrile (B), both containing 0.1% formic acid. And the column was eluted with a gradient program as follows: 0-2.0 min, 80% A; 2.0-9.0 min, 80-55% A; 9.0-13.0 min, 55% A; 13.0-14.0 min, 55%-10% A; 14.0-15.0 min, 10% A; 15.0-16.0 min, 10-80% A; 16.0-18.0 min, 80% A. An AB SCIEX Instruments 4000 hybrid triple quadrupole-liner ion trap (Q-Trap) mass spectrometer was applied to characterize NAC conjugates. MS/MS analyses were executed through an MRM-EPI (enhanced product ion) scanning in positive-ion mode (449.0→320.0 for M1 and M2; 435.0→221.0 for M3-M6; and 437.0→181.1 for M7 and M8).

Metabolizing Enzyme Inhibition Studies. To determine which P450 enzymes preferentially catalyze the metabolism of PPR, PPR was incubated with human liver microsomes in the presence of individual selective CYP inhibitors. Similar microsomal incubations as described above were conducted with minor modification that CYP inhibitors were included in microsomal mixtures besides the components above. The inhibitors applied, along with their final concentrations, were: α-naphthoflavone (10 μM for 1A2), methoxsalen (20 μM for 2A6), sulfaphenazole (20 μM for 2C9), ticlopidine (100 μM for 2B6 and 2C19), quinidine (10 μM for 2D6), disulfiram (10 μM for 2E1), and ketoconazole (10 μM for 3A) (referring to the FDA

Guidance for Industry on Drug Interaction Studies). Control group did not include the inhibitors. Sample preparation and product quantification were performed as above. P450 activities were calculated as the percentage of the control activities, each incubation was carried out three times in three separate days.

Recombinant Human P450 Incubations. Similar incubations were conducted as above microsomal study, and PPR was incubated with individual recombinant human P450 enzymes (100 nM in each incubation), including CYPs2A6, 2C9, 1A2, 2E1, 3A4, 2C19, 3A5, 2B6, and 2D6, in place of human liver microsomes. The resulting NAC adducts (M3-M8) were analyzed and quantified by LC-MS/MS. The formation of NAC adducts (%) was calculated by determination of the ratio of peak area of metabolites in individual recombinant CYP enzymes to the most abundance of the metabolites generated.

Statistical Analysis. All of the data reported represent the mean ± standard deviation (SD). Statistical evaluation was performed using unpaired *t*-test, and $*p<0.05$, $**p<0.01$, and $***p<0.001$ were accepted to be statistically significant.

Results

Overview of PPR-Mediated Time-Dependent Inhibition of CYP Enzymes. In order to define the inhibitory effect of PPR (80 μM) on seven common CYP enzymes, we first performed a quick screening study. The remaining activities of the seven CYP enzymes were measured after incubation at various time points. As illustrated in Figure 1, loss of CYPs3A and 2D6 activities was observed after 20 min incubation. The remaining enzyme activities of CYP3A and CYP2D6 were about 50% and 57%, respectively.

Time-, Concentration-, and NADPH-Dependent Inhibition of CYP3A by PPR. As shown in Figure 2A, CYP3A activity decreased with incubation time after exposure to PPR at concentrations of 5.0, 10, 20, 40, 60 or 80 μM. Specifically, exposure to PPR at 80 μM in 20 min at 37 °C resulted in a loss of approximately 50% CYP3A activity (Figure 2A). No such enzyme inactivation was observed in the absence of either PPR or NADPH (Figure 2B) under the same incubation condition.

A double-reciprocal plot (Wilson's plot) of the observed rates of inactivation (k_{obs}) and PPR concentrations above were applied to calculate kinetic constants K_I and k_{inact} (Figure 2C). K_I was obtained from the negative reciprocal of the x-axis intercept, and k_{inact} was determined by the value of the 2.3/y-axis intercept (Alvarez-Diez et al., 2004). Therefore, K_I and k_{inact} were calculated to be 30.7 μM and 0.041 min^{-1}, respectively.

Protection Effect of Competitive Inhibitor on PPR-Mediated CYP3A Inactivation. Ketoconazole was co-incubated with PPR in human liver microsomes. The protective

effect of ketoconazole increased with the increase in concentrations of ketoconazole applied (Figure 3). The residual enzymatic activity of CYP3A in the absence of ketoconazole was 47.9±5.2% at 20 min, while the remaining enzyme activities were 59.3±0.7%, 71.6±1.9%, and 81.0±1.3% in the presence of ketoconazole at concentrations of 0.01, 0.1, and 1.0 μM, respectively.

Effects of GSH and SOD/Catalase on Enzyme Inactivation. The effects of GSH and SOD/catalase on enzyme inactivation were determined by examining PPR-mediated CYP3A inactivation in the absence or presence of GSH as well as SOD/catalase. After incubation for 20 min, the remaining activities of CYP3A were 55.1±1.1% with GSH (2.0 mM) and 52.5±0.7% without GSH. SOD and catalase, scavengers of reactive oxygen species (ROS), displayed little protective effects on the inactivation of CYP3A, and the remaining enzyme activities were 53.0±3.5 % (with SOD/catalase) and 52.5±0.7 % (without SOD/catalase) after 20 min incubations.

Partition Ratio for Inactivation of CYP3A4 by PPR. Partition ratio (*P* value) is a measure of the efficiency of a mechanism-based inactivator. The *P* value was calculated by a plot of the remaining enzyme activity versus the PPR/CYP3A4 molar ratio. As shown in Figure 4, two linear regression lines with PPR/CYP3A4 as the abscissa and the remaining enzyme activity as the ordinate. The *P* value was 273 calculated from *P*+1 of 274 estimated based on the value of the intersection of two linear regression lines.

Reversibility of Inactivation. The experiment of dialysis was designed and executed

to determine the reversibility of the observed CYP3A enzyme inhibition after exposure to PPR. The changes in CYP3A activity of microsomes exposed to PPR and those treated with vehicle before and after dialysis were examined. Apparently, the observed loss of CYP3A activity was reversed by 6 h dialysis, and the enzyme activity was restored from 28.2±3.2% (pre-dialysis) to 71.9±5.2% (post-dialysis), about 43.7% of CYP3A activity was recovered.

Effect of Ferricyanide on PPR-Mediated CYP3A Inhibition. The contribution of carbene intermediate to enzyme inactivation was investigated by selective oxidation of carbene-iron complex with potassium ferricyanide. Compared with vehicle group, 39.7% of CYP3A activity was recovered when PPR-pretreated (80 μM) microsomes were incubated with $K_3Fe(CN)_6$ (2.0 mM) (Table 1).

Formation of Quinone Metabolite from PPR. Characterization of reactive metabolites of PPR was carried out in human liver microsomes supplemented with NAC as a trapping agent. A total of eight NAC conjugates (M1-M8) were found in the resulting microsomal mixture. Metabolites M1 and M2 with $[M+H]^+$ ion at *m*/*z* 449 eluted at 11.22 and 11.54 min, respectively (Figure 7B). And their mass spectra showed representative fragment ions related to the NAC moiety (Figure 7D). The product ion at *m*/*z* 320 was obtained from the neutral cleavage of the C−S bond of the NAC moiety (-129 Da). The fragment ion at *m*/*z* 407 originated from the loss of the acetyl portion (-42 Da) from *m*/*z* 449. Product ion at *m*/*z* 322 arose from the loss of the piperidine ring (-85 Da) from *m*/*z* 407. The fragment ion at *m*/*z* 135 resulted from

the cleavage of PPR portion. In addition, M1 and M2 were detected in microsomal incubations both in the absence and presence of NADPH (Figures 7A and 7B).

Another two types of NAC adducts with molecular ions *m*/*z* 435 (M3-M6) and 437 (M7, M8) were detected (Figures 8B and 9B, respectively, Schemes 1 and 2). Four peaks assigned as M3 (retention time=10.49 min), M4 (retention time=10.99 min), M5 (retention time=11.39 min), and M6 (retention time=11.72 min) (Figure 8B) showed their $[M+H]^+$ at *m*/*z* 435 in agreement with the molecular weight of DM-PPR-derived NAC conjugates. The generation of M3-M6 was NADPH-dependent (Figures 8A and 8B). MRM-EPI of ion transition at *m*/*z* 435/221 was scanned to acquire the MS/MS spectra of the four NAC conjugates. Identification of M3-M6 was based on the major fragments at *m*/*z* 306, 263, and 221 (Figure 8D). Fragment ion *m*/*z* 306 came from the characteristic neutral loss of 129 Da (the NAC moiety) from *m*/*z* 435, and fragment ion *m*/*z* 221 was derived from the loss of piperidine ring (-85 Da) from *m*/*z* 306. The product ion at *m*/*z* 263 resulted from the loss of the acetyl, carboxyl and piperidine ring of the parent ion.

In addition to M3-M6, another type of DM-PPR-derived NAC conjugates, namely M7 and M8, with retention time at 10.99 and 11.37 min (Figure 9B) were detected in the above microsomal incubations. Incubations in the absence of NADPH did not produce the two conjugates (Figure 9A). The molecular ion of conjugates M7-M8 was found to be *m*/*z* 437 which is 2 Da (2 H) higher than that of M3-M6 (*m*/*z* 435). MRM-EPI scanning (ion transition *m*/*z* 437/181) revealed representative fragment ions (Figure 9D), including *m*/*z* 308 (loss of 129 Da) associated with the indicative neutral

loss of the NAC portion, *m*/*z* 223 derived from the further loss of piperidine ring (-85 Da) from *m*/*z* 308, and *m*/*z* 181 generated from the loss of -CO (28 Da) and -CH_2 (14 Da) of *m*/*z* 223.

Chemical synthesis was carried out to verify the structure of the metabolites detected in microsomal incubations. M1-M8 were all observed in the synthetic mixture by LC-MS/MS. The resulting products showed the same chromatographic (Figures 7C, 8C, and 9C) and mass spectrometric (Figures 7E, 8E, and 9E) identities as those generated in microsomal incubations. Unfortunately, poor reaction yield and heavy impurity with similar retention time made us fail to obtain sufficient amounts of the individual products for NMR characterization.

Time- and NADPH-Dependent Inhibition of CYP3A by DM-PPR. To further probe the contribution of carbene intermediate to the inhibition of CYP3A, DM-PPR was synthesized and tested. High-resolution mass spectrometry analysis of synthetic DM-PPR revealed its $[M+H]^+$ of *m*/*z* 274.1436, consistent with the corresponding theoretical mass within 5 ppm, compared with the predicted formula (Supplemental Table 1). We succeeded in obtaining ^{1}H NMR (DMSO-d_6, 600 MHz) spectrum of synthetic DM-PPR (Supplemental Figure 1), and the proton assignment is listed in Figure 5. The signals responsible for the methylene moiety observed in ^{1}H NMR spectrum of the parent compound disappeared in the spectrum of the product.

DM-PPR at concentrations of 0 and 80 μM was incubated with human liver microsomes in the absence or presence of NADPH and was found to display time-dependent inhibition of CYP3A. NADPH was required for the enzyme inhibition

(Figure 6A). Exposure to DM-PPR at 80 μM for 20 min at 37 °C resulted in about 31.8±2.5% loss of CYP3A activity (Figures 6A and 6B), while exposure to the parent compound at the same molar concentration resulted in 50.3±2.7% loss (Figure 6B) of the enzyme activity under the same condition.

P450 Enzymes Responsible for PPR Bioactivation. To identify which P450 enzymes are mainly responsible for the bioactivation of PPR, nine human recombinant CYPs were individually incubated with PPR, NAC, and NADPH, followed by assessment of the formation of M3-M6 and M7, M8. P450 1A2 was found to be the major enzyme participating in the formation of M3-M6 and M7, M8 (Figures 10A and 11A).

Additionally, PPR was incubated with human liver microsomes fortified with NAC in the absence or presence of individual P450 enzyme inhibitors. As shown in Figures 10B and 11B, α-naphthoflavone, the inhibitors of CYP 1A2, elicited inhibitory effects on the production of M3-M6 and M7, M8. Specifically, the production of M3-M6 and M7, M8 remained at levels of 55.2±1.6%, 54.0±3.9%, 68.6±4.9%, 72.0±5.8%，53.5±6.5%, and 72.0±3.6%, respectively.

Discussion

The rapid screening experiment demonstrated that PPR caused significant loss of CYP3A and CYP2D6 activity after 20 min microsomal incubation (Figure 1). Apparently, PPR inhibited CYP3A the most, which encouraged us to investigate the interaction of PPR with CYP3A as a model enzyme.

PPR was found to cause time-, concentration-, and NADPH-dependent inhibition of CYP3A (Figures 2A and 2B). The observed requirement of NADPH for PPR-mediated CYP3A inhibition indicates that metabolic activation was involved in the enzyme inhibition. Competitive inhibitor co-incubation experiments showed that ketoconazole reduced the enzyme inactivation of CYP3A by PPR (Figure 3). This suggests that the bioactivation of PPR occurred at the active site of CYP3A, and the competitive binding of ketoconazole in the active site of the host enzyme protected the enzyme from inactivation (Moruno-Davila et al., 2001).

In consideration of reactive intermediates that release from the active site of the host enzyme and of reactive oxygen species (ROS) produced during metabolism also can contribute to enzyme inactivation, the effects of GSH and scavengers of ROS on enzyme inactivation were determined. GSH revealed minor protection against enzyme inactivation by PPR. This indicates that the reactive intermediates produced via P450-mediated metabolism resided the pocket of the host enzyme. SOD and catalase, scavengers of ROS, displayed little protective effects on the inactivation of CYP3A. That implies that ROS, if produced, was not involved in the enzyme inactivation.

Partition ratio (*P* value) is a measure to evaluate the effectiveness of a mechanism-

based inactivator. The less the value is, the more effective the inactivator. The reported *P* values of mechanism-based inactivators ranged from almost zero to several thousands (Kent et al., 2001). The observed *P* value of PPR was approximately 273 (Figure 4), which can be classified as a moderately efficient inactivator of CYP3A4.

Dialysis experiments were conducted to define the interaction of the metabolite of PPR with host enzyme CYP3A. Apparently, dialysis restored the enzyme activity of CYP3A, indicating that the binding mode of the enzyme to the metabolite was non-covalent.

MDP compounds may be metabolized to carbene intermediates mediated by P450 enzymes, and the resulting carbene may coordinate with the iron of the heme, resulting in inhibition of the host enzymes (Buening and Franklin, 1976; Muakkassah et al., 1982). Potassium ferricyanide can reportedly reverse the carbene-mediated inhibition by selective oxidation and dissociation of carbene-heme-iron-porphyrin complexes (Buening and Franklin, 1976). The addition of $K_3Fe(CN)_6$ showed protective effect on the inhibition of CYP3A by PPR in the incubation (Table 1), indicating that the formation of carbene-iron complex was possibly involved in the CYP3A inactivation.

Alternatively, the resulting carbene may be converted to the corresponding formate ester. The formate ester may be hydrolyzed to catechol and further oxidized to the corresponding *ortho*-quinone (Scheme 1) (Murray, 2000). As expected, we succeeded in the detection of the NAC conjugate derived from the putative quinone intermediate in human liver microsomal incubations (Figure 8). In addition, NAC conjugates M3-M8 were detected in human liver microsomal incubations with synthetic DM-PPR

(Supplemental Figures 3A and 3B). This suggests P450-mediated formation of the quinone intermediate proposed in Scheme 1. To determine the contribution of the quinone intermediate in PPR-mediated CYP3A inactivation, we evaluated the inhibitory effect of DM-PPR and found that DM-PPR showed weak enzyme inactivation relative to that caused by PPR (Figure 6). Whether the enzyme inhibition by DM-PPR is reversible was determined by dialysis. As expected, exhaustive dialysis failed to restore the DM-PPR inhibited CYP3A activity (the residual CYP3A activities were 46.7±7.4% without dialysis and 52.8±3.9% with dialysis). Taken together, the observed CYP3A inactivation resulted not only from carbene-mediated iron coordination but also from quinone-derived protein modification.

Structurally, PPR is a Michael acceptor (unsaturated ketone). As expected, two NAC conjugates (M1 and M2) were detected in human liver microsomal incubations, possibly resulting from 1,4- and 1,6-addition (Scheme 1). Additionally, cysteine conjugates were observed in PPR-exposed recombinant CYP3A4 after proteolytic digestion (Supplemental Figure 2). Thus, we cannot exclude the possibility that the observed enzyme inactivation arose from non-specific covalent modification of CYP3A via Michael addition. This prompted us to determine the potential involvement of the non-specific modification in the enzyme inactivation. As a result, we failed to see the enzyme inactivation in the absence of NADPH. This suggests that the non-specific protein addition, if it took place, did not necessarily cause enzyme inactivation.

Both recombinant and microsomal inhibition studies verified that CYP1A2 was the primary enzyme participating in the bioactivation of PPR measured by monitoring

the formation of NAC adducts derived from the quinone intermediate (M3-M8) (Figures 10 and 11). Methoxsalen was reportedly an inhibitor of both CYPs 2A6 and 1A2 (Ono et al., 1996). That is probably why the results obtained from the CYP2A6 recombinant incubations and microsomal inhibition incubations did not quite match each other. Interestingly, CYP1A2 was found to be the major enzyme which mediated the bioactivation of PPR, but PPR caused significant inactivation of CYP3A and slight inactivation of CYP2D6. Reactive metabolites generated in the active site of CYP3A selectively inactivated the host enzymes, which made their activity survive not long enough to produce many metabolites. Additionally, reactive metabolites generated in the active site of enzymes did not necessarily result in inactivating the host enzymes, and it also depends on the availability of nucleophilic amino acid residues at their active sites and the suitable distance between the resulting reactive intermediate and the targeting nucleophilic amino acid residues of the host enzymes. For some reason, the reactive metabolite generated *in situ* was unable to modify the amino acid residue(s) in the active site of CYP1A2, sequentially escaped from the host enzymes, and trapped by NAC. Whether PPR is a mechanism-based inactivator of CYP2D6 needs further investigation.

In summary, PPR quasi-irreversibly inhibited CYP3A, and biotransformation was required for the enzyme inactivation. Both the carbene and *ortho*-quinone reactive intermediates are involved in the inactivation of CYP3A.

Authorship Contributions:

Participated in research design: Cui, Zheng, and Peng.

Conducted experiments: Cui, Wang, Tian, and Zhang.

Performed data analysis: Cui.

Wrote or contributed to the writing of the manuscript: Cui and Zheng.

References

Alvarez-Diez TM and Zheng J (2004) Mechanism-Based Inactivation of Cytochrome P450 3A4 by 4-Ipomeanol. *Chem Res Toxicol* **17**(2): 150-157.

Buening MK and Franklin MR (1976) SKF 525-A inhibition, induction, and 452-nm complex formation. *Drug Metab Dispos* **4**(3): 244.

Bang JS, Oh DH, Choi HM, Sur BJ, Lim SJ, Kim JY, Yang HI, Yoo MC, Hahm DH, and Kim KS (2009) Anti-inflammatory and antiarthritic effects of piperine in human interleukin 1β-stimulated fibroblast-like synoviocytes and in rat arthritis models. *Arthritis Res Ther* **11**(2): R49.

Bae GS, Kim MS, Jung WS, Seo SW, Yun SW, Kim SG, Park RK, Kim EC, Song HJ, and Park SJ (2010) Inhibition of lipopolysaccharide-induced inflammatory responses by piperine. *Eur J Pharmacol* **642**(1): 154-162.

Bukhari I.A, Alhumayyd MS, Mahesar AL, and Gilani AH (2013) The analgesic and anticonvulsant effects of piperine in mice. *J Physiol Pharmacol* **64**(6): 789-794.

Casida JE (1970) Mixed-function oxidase involvement in the biochemistry of insecticide synergists. *J Agric Food Chem* **18**(5): 753-772.

Chonpathompikunlert P, Wattanathorn J, and Muchimapura S (2010) Piperine, the main alkaloid of Thai black pepper, protects against neurodegeneration and cognitive impairment in animal model of cognitive deficit like condition of Alzheimer's disease. *Food Chem Toxicol* **48**(3): 798-802.

Gupta RA, Motiwala MN, Dumore NG, Danao KR, and Ganjare AB (2015) Effect of piperine on inhibition of FFA induced TLR4 mediated inflammation and amelioration

of acetic acid induced ulcerative colitis in mice. *J Ethnopharmacol* **164**: 239-246.

Gong FY, Cui LF, Zhang XN, Zhan XB, Gong X, and Wen Y (2017) Piperine ameliorates collagenase-induced Achilles tendon injury in the rat. *Connect Tissue Res* **59**(6): 21-29.

Hutzler JM, Melton RJ, Rumsey JM, Schnute ME, Locuson CW, and Wienkers LC (2006) Inhibition of cytochrome P450 3A4 by a pyrimidineimidazole: evidence for complex heme interactions. *Chem Res Toxicol* **19**: 1650-1659.

Hutzler JM, Meltonm RJ, Rumsey JM, Thompson DC, Rock DA, and Wienkers LC (2008) Assessment of the metabolism and intrinsic reactivity of a novel catechol metabolite. *Chem Res Toxicol* **21**: 1125-1133.

Hong Y, Chia YMF, Yeo RH, Venkatesan G, Koh SK, Chai CLL, Zhou L, Kojodjojo P, and Chan ECY (2015) Inactivation of human cytochrome P450 3A4 and 3A5 by dronedarone and N-desbutyl dronedarone. *Mol Phanmacol* **89**(1): 1-13.

Johri RK and Zutshi U (1992) An Ayurvedic formulation 'Trikatu' and its constituents. *J Ethnopharmacol* **37**(2): 85-91.

Kent UM, Jushchyshyn MI, and Hollenberg PF (2001) Mechanism-based inactivators as probes of cytochrome P450 structure and function. *Curr Drug Metab* **2**(3): 215-243.

Kumar A, Khan IA, Koul S, Koul JL, Taneja SC, Ali I, Ali F, Sharma S, Mirza Z.M, Kumar M, Sangwan PL, Gupta P, Thota N, and Qazi GN (2008) Novel structural analogues of piperine as inhibitors of the NorA efflux pump of Staphylococcus aureus. *J Antimicrob Chemother* **61**(6): 1270-1276.

Katiyar SS, Muntimadugu E, Rafeeqi TA, Domb AJ, and Khan W (2016) Co-delivery of rapamycin- and piperine-loaded polymeric nanoparticles for breast cancer treatment. *Drug Deliv* **23**(7): 2608-2616.

Lin JH and Lu AY (1998) Inhibition and induction of cytochrome P450 and the clinical implications. *Clin Pharmacokinet* **35**(5): 361-390.

Liu YT, Hao HP, Liu CX, Wang GJ, and Xie HG (2007) Drugs as CYP3A probes, inducers, and inhibitors. *Drug Metab Rev* **39**(4): 699-721.

Lee JY, Lee SY, Oh SJ, Lee KH, Jung YS, and Kim SK (2012) Assessment of drug-drug interactions caused by metabolism-dependent cytochrome P450 inhibition. *Chem-Biol Interact* **198**(1-3): 49-56.

Muakkassah SF, Bidlack WR, and Yang WC (1982) Reversal of the effects of isoniazid on hepatic cytochrome P-450 by potassium ferricyanide. *Biochem Pharmacol* **31**: 249-251.

Murray M (2000) Mechanisms of inhibitory and regulatory effects of methylenedioxyphenyl compounds on cytochrome P450-dependent drug oxidation. *Curr Drug Metab* **1**(1): 67-84.

Moruno-Davila MA, Garrido-del Solo C, Garcia-Moreno M, Havsteen BH, Garcia-Sevilla F, Garcia-Canovas F, and Varon R (2001) Kinetic analysis of enzyme systems with suicide substrate in the presence of a reversible competitive inhibitor, tested by simulated progress curves. *Int J Biochem Cell Biol* **33(**2):181-191.

Murunikkara V, Pragasam SJ, Kodandaraman G, Sabina EP, and Rasool M (2012) Anti-inflammatory effect of piperine in adjuvant-induced arthritic rats - a biochemical

approach. *Inflamm* **35**(4): 1348-1356.

Murray GI, Barnes TS, Sewell HF, Ewen SW, Melvin WT, and Burke MD (2012) The immunocytochemical localisation and distribution of cytochrome P-450 in normal human hepatic and extrahepatic tissues with a monoclonal antibody to human cytochrome P-450. *Brit J Clin Pharmacol* **25**(4): 465-475.

Ono S, Hatanaka T, Hotta H, Satoh T, Gonzalez FJ, and Tsutsui M (1996) Specificity of substrate and inhibitor probes for cytochrome P450s: evaluation of in vitro metabolism using cDNA-expressed human P450s and human liver microsomes. *Xenobiotica* **26**(7): 681-693.

Ohnishi A, Matsuo H, Yamada S, Takanaga H, Morimoto S, Shoyama Y, Ohtani H, and Sawada Y (2010) Effect of furanocoumarin derivatives in grapefruit juice on the uptake of vinblastine by Caco-2 cells and on the activity of cytochrome P450 3A4. *Brit J Pharmacol* **130**(6): 1369-1377.

Parkinson A, Kazmi F, Buckley DB, Yerino P, Paris BL, Holsapple J, Toren P, Otradovec SM, and Ogilvie BW (2011). An evaluation of the dilution method for identifying metabolism-dependent inhibitors of cytochrome P450 enzymes. *Drug Metab Dispos* **39**(8): 1370-1387.

Rendic S and Di Carlo FJ (1997) Human cytochrome P450 enzymes: a status report summarizing their reactions, substrates, inducers, and inhibitors. *Drug Metab Rev* **29**(1-2): 413-580.

Rama Subba Rao V, Suresh G, Ranga Rao R, Suresh Babu K, Chashoo G, Saxena A, and Madhusudana Rao J (2012) Synthesis of piperine–amino acid ester conjugates

and study of their cytotoxic activities against human cancer cell lines. *Med Chem Res* **21**(1): 38-46.

Salminen KA, Meyer A, Imming P, and Raunio H (2011) CYP2C19 progress curve analysis and mechanism-based inactivation by three methylenedioxyphenyl compounds. *Drug Metab Dispos* **39**(12): 2283-2289.

Samra YA, Said HS, Elsherbiny NM, Liou GI, El-Shishtawy MM, and Eissa LA (2016) Cepharanthine and piperine ameliorate diabetic nephropathy in rats: role of NF-κB and NLRP3 inflammasome. *Life Sci* **157**: 187-199.

Taxak N, Patel B, and Bharatam PV (2013) Carbene generation by cytochromes and electronic structure of heme-iron-porphyrin-carbene complex: a quantum chemical study. *Inorg Chem* **52**: 5097-5109.

Tasleem F, Azhar I, Ali SN, Perveen S, and Mahmood ZA (2014) Analgesic and anti-inflammatory activities of *piper nigrum*, L. *Asian Pac J Trop Med* **7**(1): S461-S468.

Usia T, Watabe T, Kadota S, and Tezuka Y (2005) Metabolite-cytochrome P450 complex formation by methylenedioxyphenyl lignans of piper cubeba: mechanism-based inhibition. *Life Sci* **76**(20): 2381-2391.

Umadevi P, Deepti K, and Venugopal DVR (2013) Synthesis, anticancer and antibacterial activities of piperine analogs. *Med Chem Res* **22**(11): 5466-5471.

Umar S, Sarwar AMG, Umar K, Ahmad N, Sajad M, Ahmad S, Katiyar CK, and Khan HA (2013) Piperine ameliorates oxidative stress, inflammation and histological outcome in collagen induced arthritis. *J Cell Immunol* **284**(1-2): 51-59.

VandenBrink BM and Isoherranen N (2010) The role of metabolites in predicting drug-

drug interactions: Focus on irreversible P450 inhibition. *Curr Opin Drug Discov Dev* **13**(1): 66-77.

Wangensteen H, Molden E, Christensen H, and Malterud KE (2003) Identification of epoxybergamottin as a CYP3A4 inhibitor in grapefruit peel. *Eur J Clin Pharmacol* **58**(10): 663-8.

Watanabe A, Nakamura K, Okudaira N, Okazaki O, and Sudo KI (2007) Risk assessment for drug-drug interaction caused by metabolism-based inhibition of CYP3A using automated in vitro assay systems and its application in the early drug discovery process. *Drug Metab Dispos* **35**(7): 1232-1238.

Wattanathorn J, Chonpathompikunlert P, Muchimapura S, Priprem A, and Tankamnerdthai O (2008) Piperine, the potential functional food for mood and cognitive disorders. *Food Chem Toxicol* **46**(9): 3106-3110.

Yang AH, He X, Chen JX, He LN, Jin CH, Wang LL, Zhang FL, and An LJ (2015) Identification and characterization of reactive metabolites in myristicin-mediated mechanism-based inhibition of CYP1A2. *Chem Biol Interact* **237**: 133-140.

Zarai Z, Boujelbene E, Ben Salem N, Gargouri Y, and Sayari A (2013) Antioxidant and antimicrobial activities of various solvent extracts, piperine and piperic acid from *Piper nigrum*. *LWT - Food Sci and Technol* **50**(2): 634-641.

Footnotes. This work was supported in part by the National Natural Science Foundation of China [Grant 81830104, 81430086, 81773813, U1812403].

Conflict of interest. The authors declare that there are no conflicts of interest.

Scheme Legends

Scheme 1. Proposed pathways for the generation of reactive intermediate(s) and NAC conjugates derived from PPR.

Scheme 2. Proposed mechanisms for the formation of NAC conjugates M3-M8.

Figure Legends

Figure 1. Quick screening of time-dependent inhibition of cytochromes P450 enzymes by PPR. PPR at concentrations of 0 (■) or 80 (◆) μM, human liver microsomes (0.5 mg protein/mL), and NADPH (1.0 mM) were incubated at 37 °C for 0, 5, 10, and 20 min. The residual enzymatic activities at 0 min were normalized to 100%. Data represent the mean±SD (n=3). Comparisons were made using an unpaired *t*-test. * indicates the significance of the remaining enzyme activity of experimental groups with respect to that of control at the same time point (20 min) of incubations. Levels are considered significant at *p<0.05, **p<0.01, and ***p<0.001; ns, not significant.

Figure 2. A: Time- and concentration-dependent inhibition of CYP3A by PPR. PPR at concentrations of 0 (■), 5 (●), 10 (▲), 20 (▼), 40 (◆), 60(★), and 80 (○) μM was incubated with human liver microsomes (0.5 mg protein/mL) fortified with NADPH (1.0 mM) at 37 °C for 0, 5, 10, and 20 min. B: NADPH-dependent inactivation of CYP3A4 by PPR. Human liver microsomes (0.5 mg/mL) were incubated with vehicle (■) or PPR (80 μM) in the absence (▼) or presence (★) of NADPH. C: Wilson's plot. k_{obs} values were calculated from the slope of the regression

lines shown in A. Data represent the mean±SD (n=3). * indicates the significance of the remaining enzyme activity of experimental groups with respect to that of control at the same time point (20 min) of incubations. $ indicates the significance of the remaining enzyme activity of experimental groups at various incubation times, compared with that at 0 min under the same incubation condition. # indicates the significance of the remaining enzyme activity in the presence of NADPH, compared with that in the absence of NADPH under the same incubation condition. Levels are considered significant at $^{*/\$/\#}p<0.05$, $^{**/\$\$/\#\#}p<0.01$, and $^{***/\$\$\$/\#\#\#}p<0.001$; ns, not significant.

Figure 3. Effect of competitive inhibitor on inactivation of CYP3A by PPR. Human liver microsomes (0.5 mg protein/mL) were incubated with vehicle (■) or PPR (80 μM) supplemented with ketoconazole at concentrations of 0 (★), 0.01 (◆), 0.1 (▲), or 1.0 (●) μM. Data represent the mean±SD (n=3). * indicates the significance of the remaining enzyme activity of experimental groups with respect to that of control at the same time point (20 min) of incubations. Levels are considered significant at $*p<0.05$, $**p<0.01$, and $***p<0.001$.

Figure 4. Partition ratio of CYP3A4 inactivation by PPR. CYP3A4 (50 nM) was incubated with PPR at designed concentrations (0, 2, 5, 10, 20, 40, 60, 80, or 100 μM). The extrapolated P+1 value was determined from the point of intersection to the abscissa. Data represent the mean±SD (n=3).

Figure 5. Chemical structure and ^{1}H NMR chemical shifts of DM-PPR.

Figure 6. A：Time- and NADPH-dependent inhibition of CYP3A by DM-PPR (80 μM). Human liver microsomes (0.5 mg protein/mL) were incubated with vehicle (■), or DM-PPR (80 μM) in the absence (▲) or presence (◆) of NADPH at 37 °C for 0, 5, 10, and 20 min. B: human liver microsomes (0.5 mg protein/mL) were incubated with vehicle (■), DM-PPR (80 μM) (◆), or PPR (80 μM) (★) in the presence of NADPH. The residual enzymatic activities at 0 min were normalized to 100%. Data represent the mean ± SD (n=3). * indicates significance of the remaining enzyme activity of experimental groups with respect to that of control at the same time point (20 min) of incubations. In Figure A, # indicates the significance of the remaining activity in the presence of NADPH, compared with that in the absence of NADPH under the same incubation condition, while in Figure B, # indicates the significance of the remaining activity of the incubation containing DM-PPR (80 μM), compared with that of PPR (80 μM) in the presence of NADPH at the same condition. $*^{/\#}p<0.05$, $**^{/\#\#}p<0.01$, and $***^{/\#\#\#}p<0.001$ are considered significantly different; ns, not significant.

Figure 7. Mass spectrometric characterization of metabolites M1 and M2. Extracted ion (*m/z* 449.0/320.0 for M1 and M2) chromatograms obtained from LC-MS/MS analysis of incubations containing PPR, human liver microsomes, and NAC in the absence (A) or presence of NADPH (B). C: Extracted ion chromatograms obtained from LC-MS/MS analysis of synthetic M1 and M2. D: MS/MS spectra of M1 and M2 generated in microsomal incubations. E: MS/MS spectra of synthetic M1 and M2.

Figure 8. Mass spectrometric characterization of DM-PPR-derived NAC conjugates

M3-M6. Extracted ion (*m/z* 435.0/221.0 for M3-M6) chromatograms obtained from LC-MS/MS analysis of incubations containing PPR, human liver microsomes, and NAC in the absence (A) or presence of NADPH (B). C: Extracted ion chromatograms obtained from LC-MS/MS analysis of synthetic M3-M6. D: MS/MS spectra of M3-M6 generated in microsomal incubations. E: MS/MS spectra of synthetic M3-M6.

Figure 9. Mass spectrometric characterization of DM-PPR-derived NAC conjugates M7 and M8. Extracted ion (*m/z* 437.0/181.0 for M7 and M8) chromatograms obtained from LC-MS/MS analysis of incubations containing PPR, human liver microsomes, and NAC in the absence (A) or presence of NADPH (B). C: Extracted ion chromatograms obtained from LC-MS/MS analysis of synthetic M7 and M8. D: MS/MS spectra of M7 and M8 generated in microsomal incubations. E: MS/MS spectra of synthetic M7 and M8.

Figure 10. P450 enzymes responsible for the generation of M3-M6 *in vitro*. A: Rates of M3-M6 formation in incubations containing PPR, individual recombinant P450 enzymes, NAC, and NADPH. B: Effects of selective P450 inhibitors on the generation of M3-M6. PPR was incubated with human liver microsomes, NAC and NADPH in the absence (control) or presence of individual P450 enzyme inhibitors. Data represent the mean±SD (n=3). *, #, $, and % indicate the significance of the amount of M3-M6 produced in experimental groups, compared with that of the control, respectively. Comparisons were made using unpaired *t*-test. $^{*/\#/\$/\%}p<0.05$, $^{**/\#\#/\$\$/\%\%}p<0.01$, and $^{***/\#\#\#/\$\$\$/\%\%\%}p<0.001$ are considered significantly different.

Figure 11. P450 enzymes responsible for the generation of M7 and M8 *in vitro*. A: Rates of M7 and M8 formation in incubations containing PPR, individual recombinant P450 enzymes, NAC, and NADPH. B: Effects of selective P450 inhibitors on the generation of M7 and M8. PPR was incubated with human liver microsomes, NAC, and NADPH in the absence (control) or presence of individual P450 enzyme inhibitors. Data represent the mean±SD (n=3). * and # indicate the significance of the amount of M7 and M8 produced in experimental groups, compared with that of the control, respectively. Comparisons were made using unpaired *t*-test. $*^{/\#}p<0.05$, $**^{/\#\#}p<0.01$, and $***^{/\#\#\#}p<0.001$ are considered significantly different.

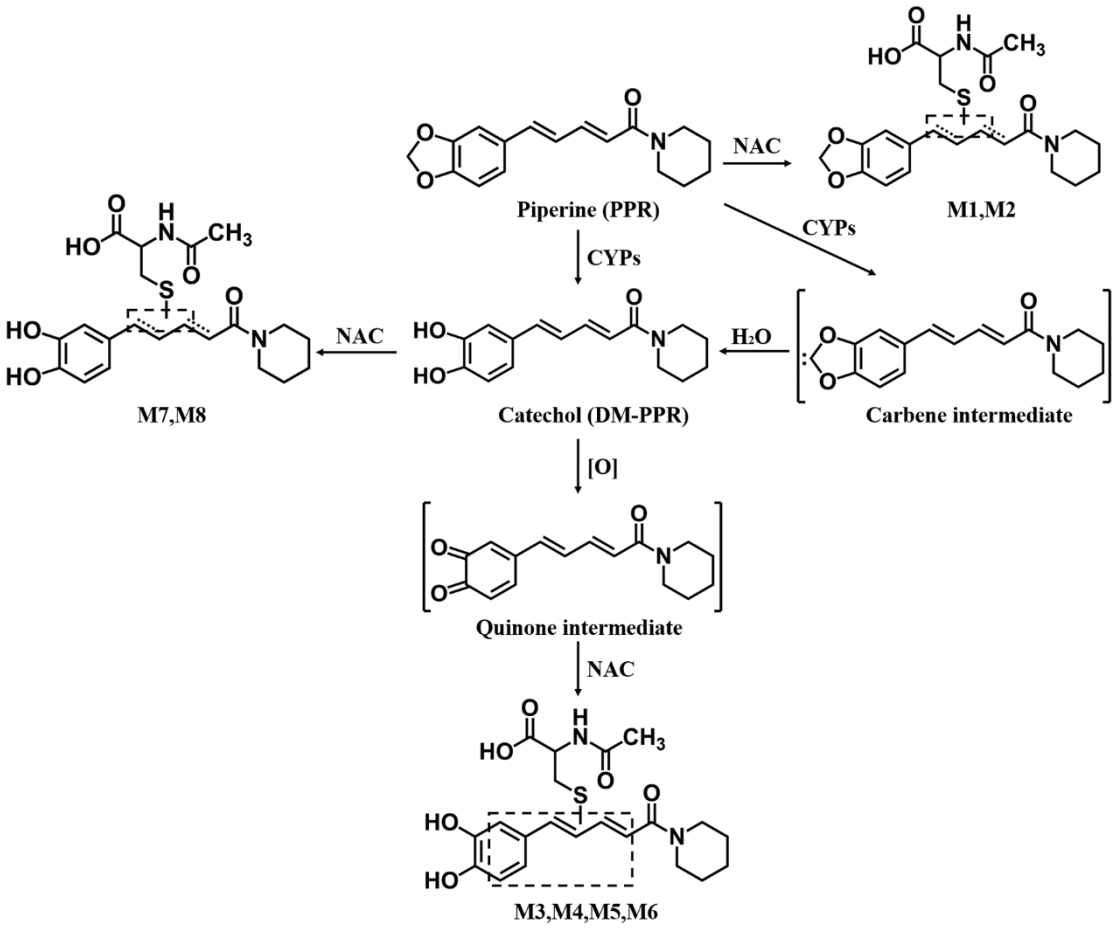
Piperine (PPR)
NAC
M1,M2
CYPs
CYPs
M7,M8
NAC
Catechol (DM-PPR)
H2O
Carbene intermediate
[O]
Quinone intermediate
NAC
M3,M4,M5,M6

Scheme 1

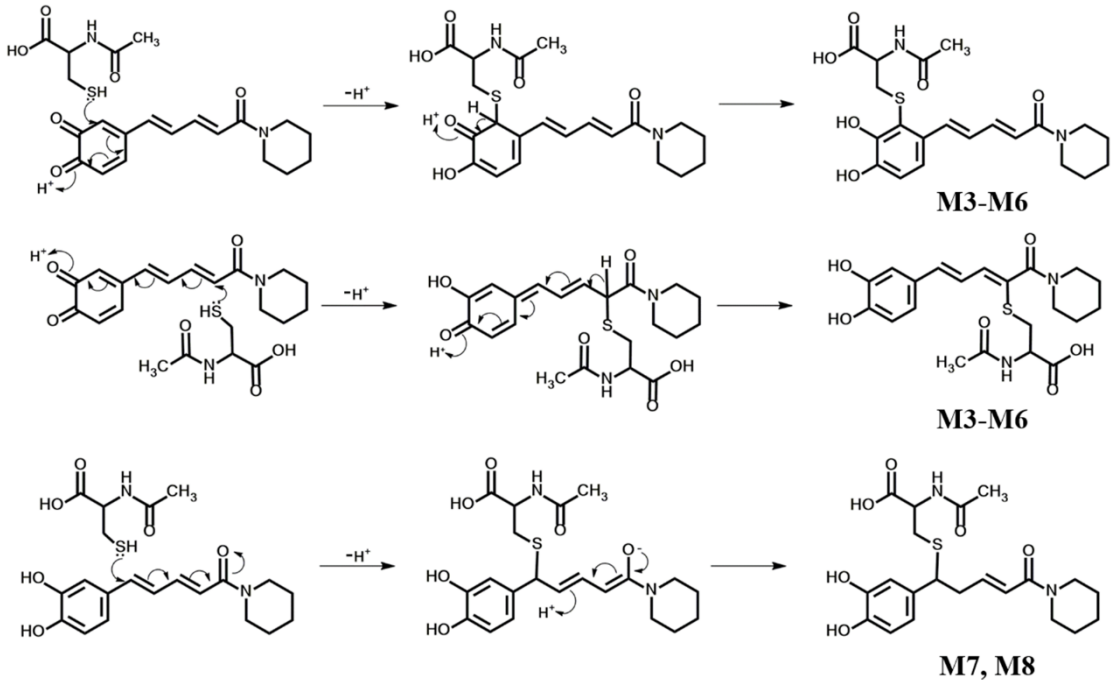

Scheme 2

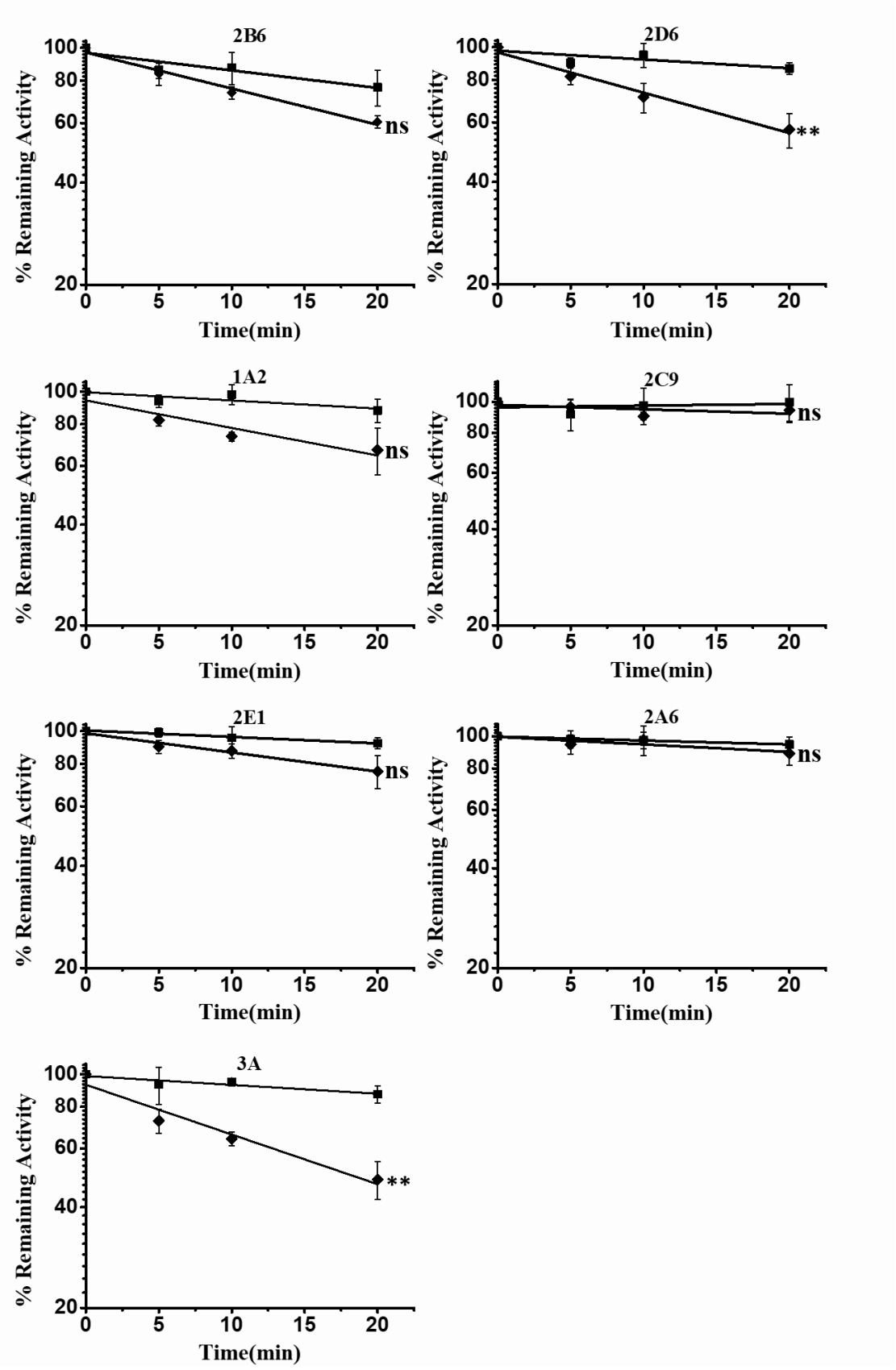
2B6
% Remaining Activity
Time(min)
ns
2D6
**
1A2
ns
2C9
ns
2E1
ns
2A6
ns
3A
**

Figure 1

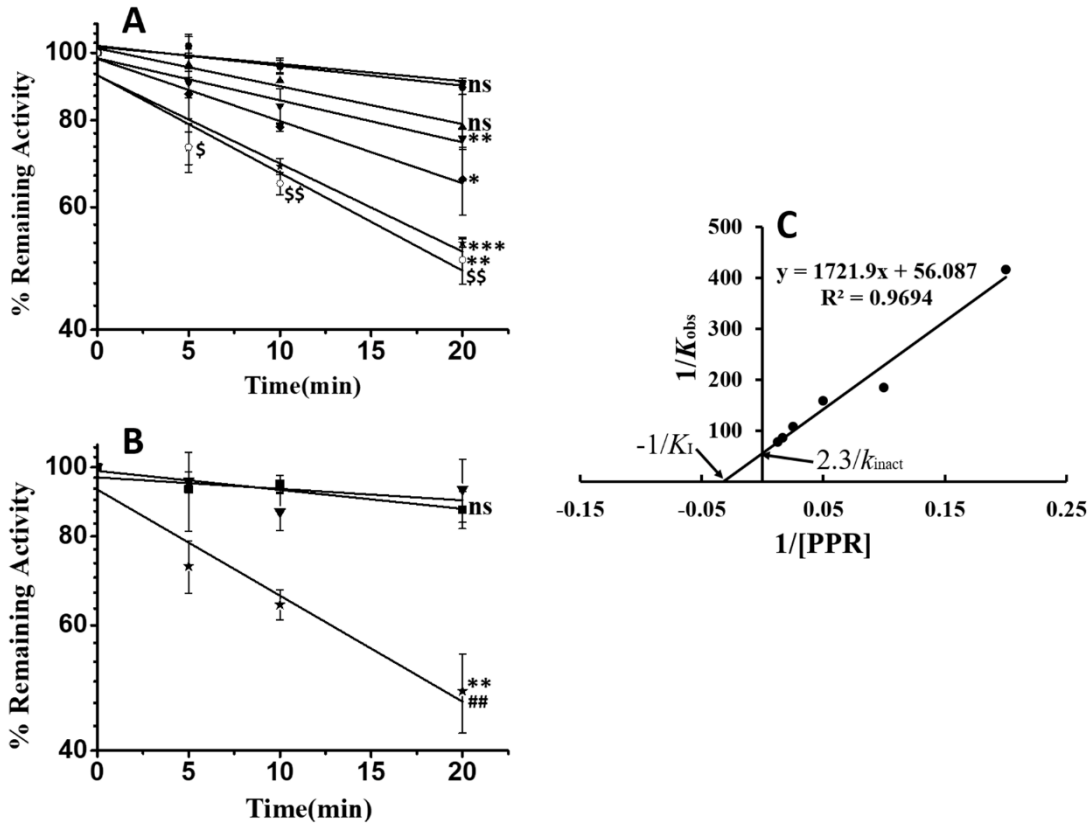
A
% Remaining Activity
Time(min)
ns
ns
**
*
***
**
$
$$
$$
B
% Remaining Activity
Time(min)
ns
**
##
C
y = 1721.9x + 56.087
R² = 0.9694
1/Kobs
-1/KI
2.3/kinact
1/[PPR]

Figure 2

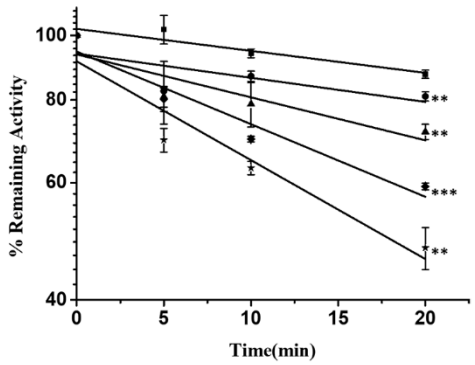

Figure 3

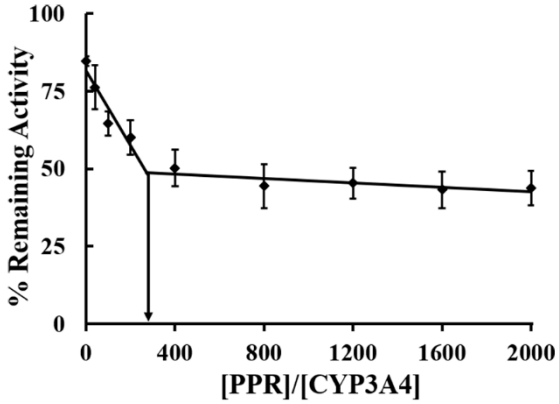
100
75
50
25
0
% Remaining Activity
0
400
800
1200
1600
2000
[PPR]/[CYP3A4]

Figure 4

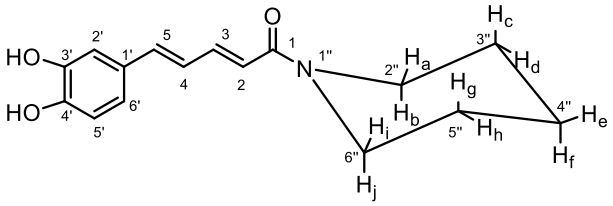

Proton	Proton Chemical Shift(ppm)	*J* (Hz)
HO-4'	9.29(1H, s)	-
HO-3'	9.05(1H, s)	-
H-3	7.22-7.18(1H, ddd)	14.6, 7.3, 3.0
H-2'	6.91(1H, d)	2.0
H-6'	6.80-6.79(1H, dd)	2.0, 8.2
H-5	6.78(1H, d)	4.3
H-4	6.77(1H, s)	-
H-5'	6.72-6.71(1H, d)	8.1
H-2	6.67-6.65(1H, d)	14.6
Ha, Hi	3.52(2H, s)	-
Hb, Hj	or 3.49(2H, s)	-
He, Hf	1.61-1.57(2H, m)	-
Hc, Hg	1.49(2H, s)	-
Hd, Hh	or 1.45(2H, s)	-

Figure 5

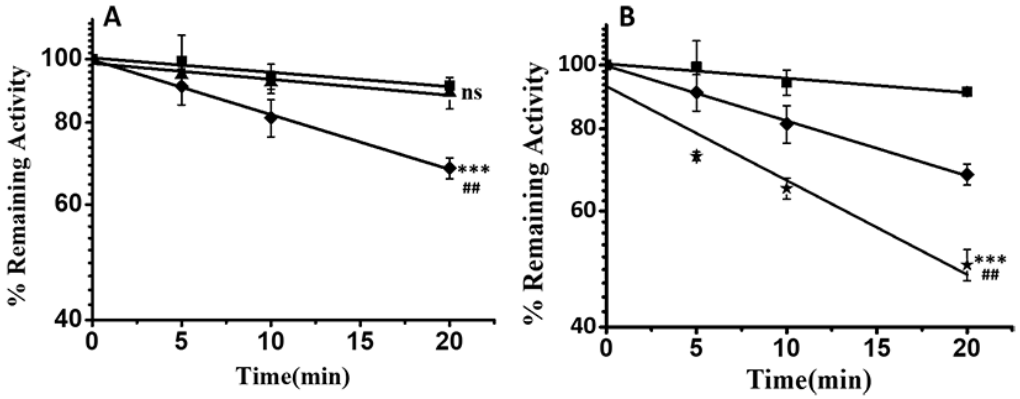
A
% Remaining Activity
100
80
60
40
0
5
10
15
20
Time(min)
ns
***
##
B
% Remaining Activity
100
80
60
40
0
5
10
15
20
Time(min)
***
##

Figure 6

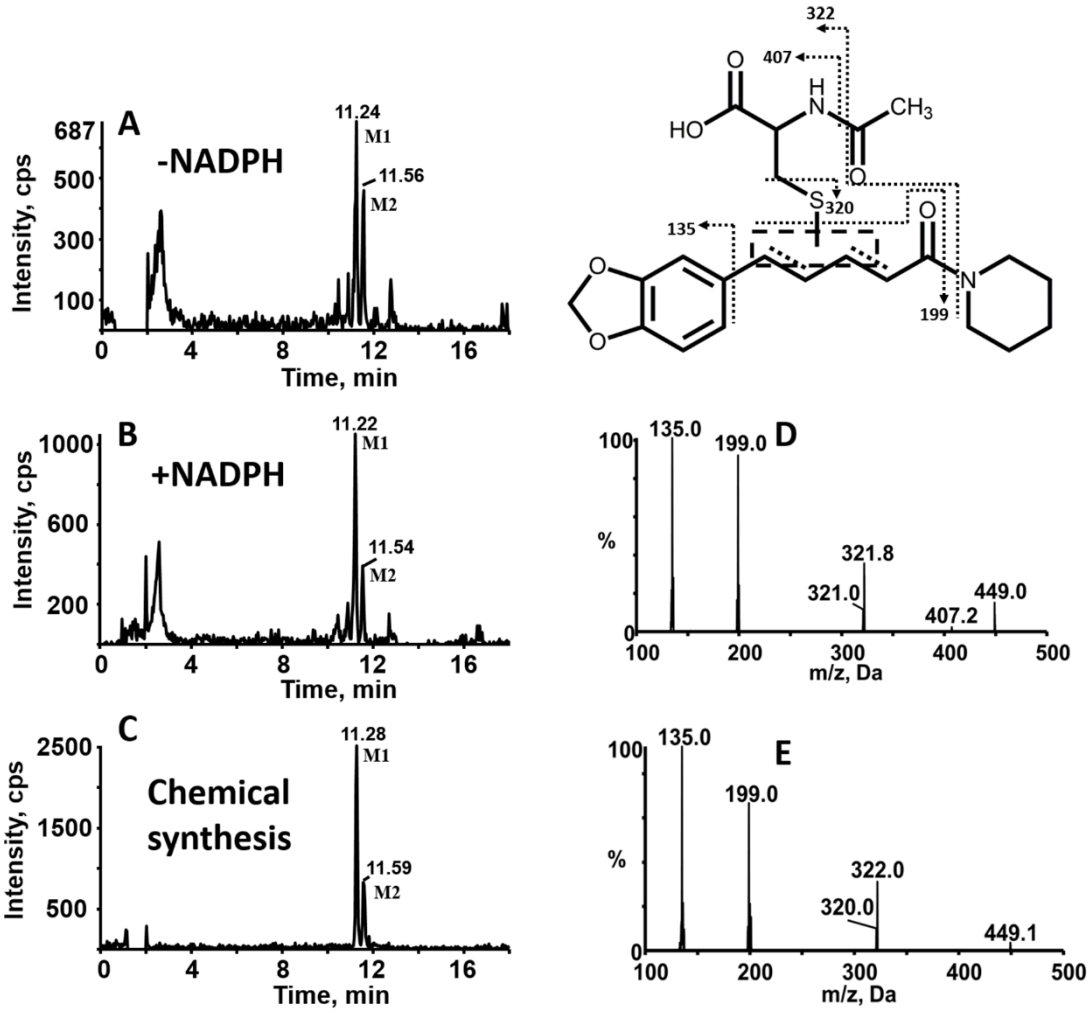
A
-NADPH
11.24
M1
11.56
M2
Intensity, cps
687
500
300
100
0
4
8
12
16
Time, min
B
+NADPH
11.22
M1
11.54
M2
1000
600
200
C
Chemical synthesis
11.28
M1
11.59
M2
2500
1500
500
322
407
135
199
320
HO
O
H
N
CH3
S
D
135.0
199.0
321.8
321.0
449.0
407.2
100
%
m/z, Da
E
322.0
320.0
449.1

Figure 7

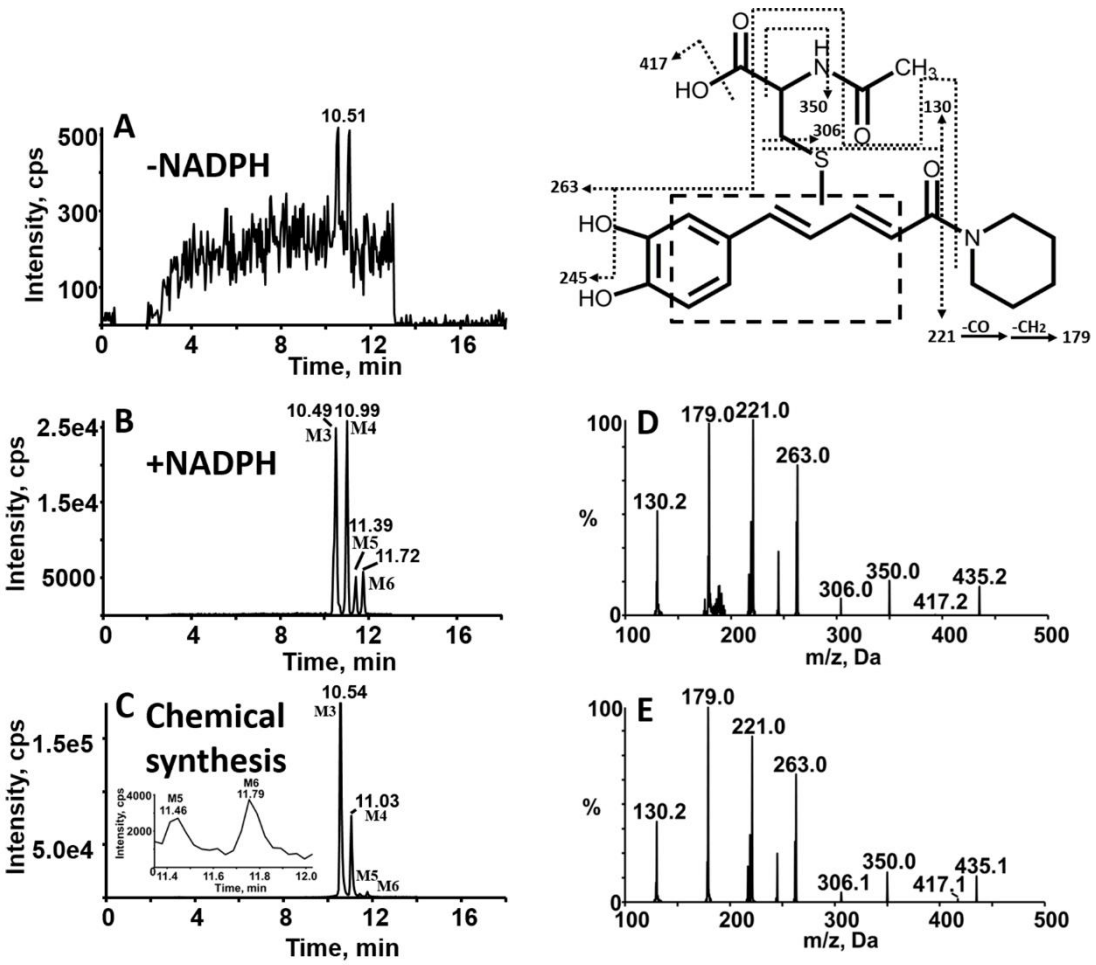
A
-NADPH
10.51
Intensity, cps
Time, min
B
+NADPH
10.49
M3
10.99
M4
11.39
M5
11.72
M6
C
Chemical synthesis
10.54
M3
11.03
M4
M5
M6
M5 11.46
M6 11.79
D
179.0
221.0
263.0
130.2
306.0
350.0
417.2
435.2
m/z, Da
E
179.0
221.0
263.0
130.2
306.1
350.0
417.1
435.1
417
350
306
130
263
245
221
-CO
-CH2
179

Figure 8

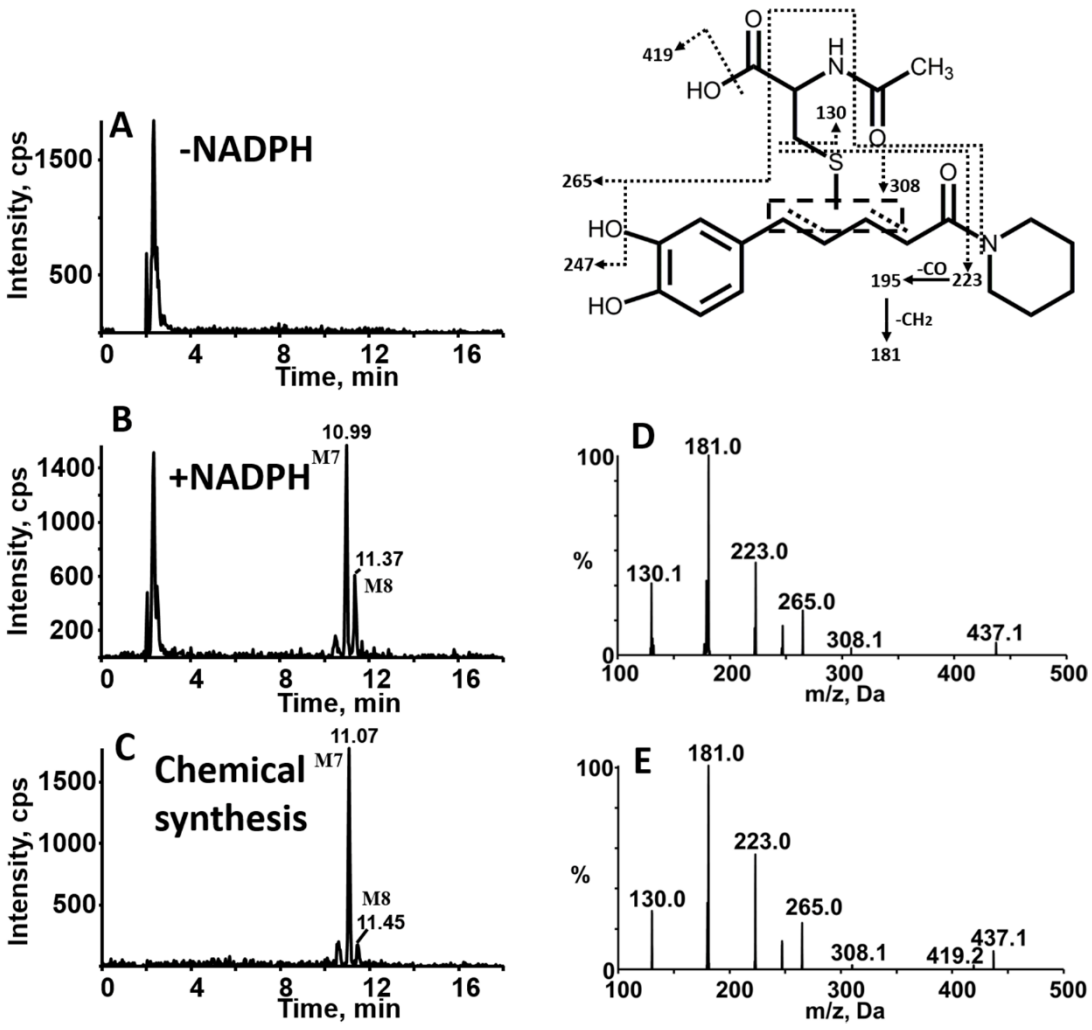
A
-NADPH
Intensity, cps
1500
500
0
4
8
12
16
Time, min
B
+NADPH
10.99
M7
11.37
M8
1400
1000
600
200
C
Chemical synthesis
11.07
M7
M8
11.45
D
181.0
223.0
130.1
265.0
308.1
437.1
100
%
m/z, Da
E
181.0
223.0
130.0
265.0
308.1
419.2
437.1
419
265
247
130
308
195
223
181
-CO
-CH2
HO
CH3
O
N
H
S

Figure 9

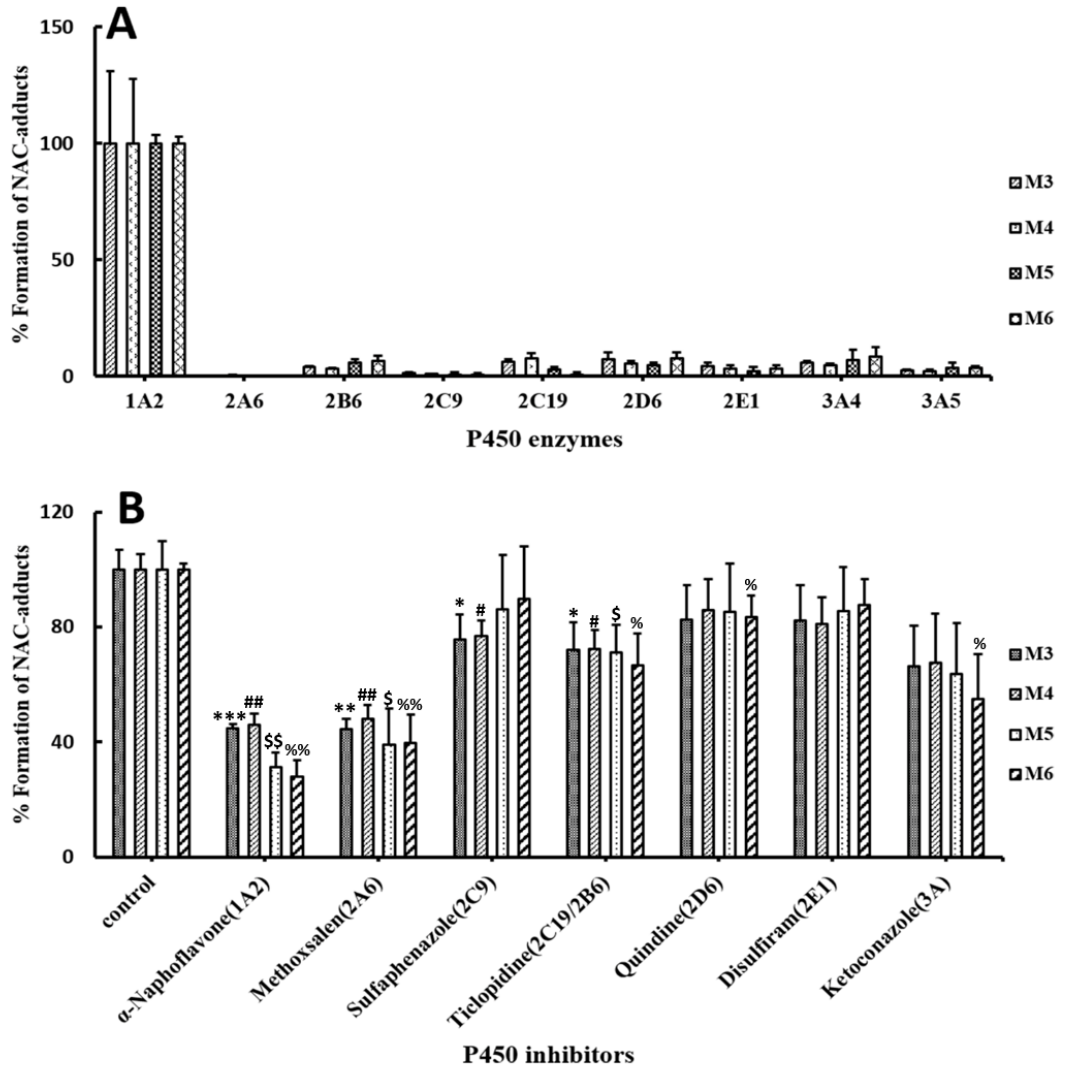
A
% Formation of NAC-adducts
150
100
50
0
M3
M4
M5
M6
1A2
2A6
2B6
2C9
2C19
2D6
2E1
3A4
3A5
P450 enzymes
B
% Formation of NAC-adducts
120
80
40
0
control
α-Naphoflavone(1A2)
Methoxsalen(2A6)
Sulfaphenazole(2C9)
Ticlopidine(2C19/2B6)
Quindine(2D6)
Disulfiram(2E1)
Ketoconazole(3A)
P450 inhibitors

Figure 10

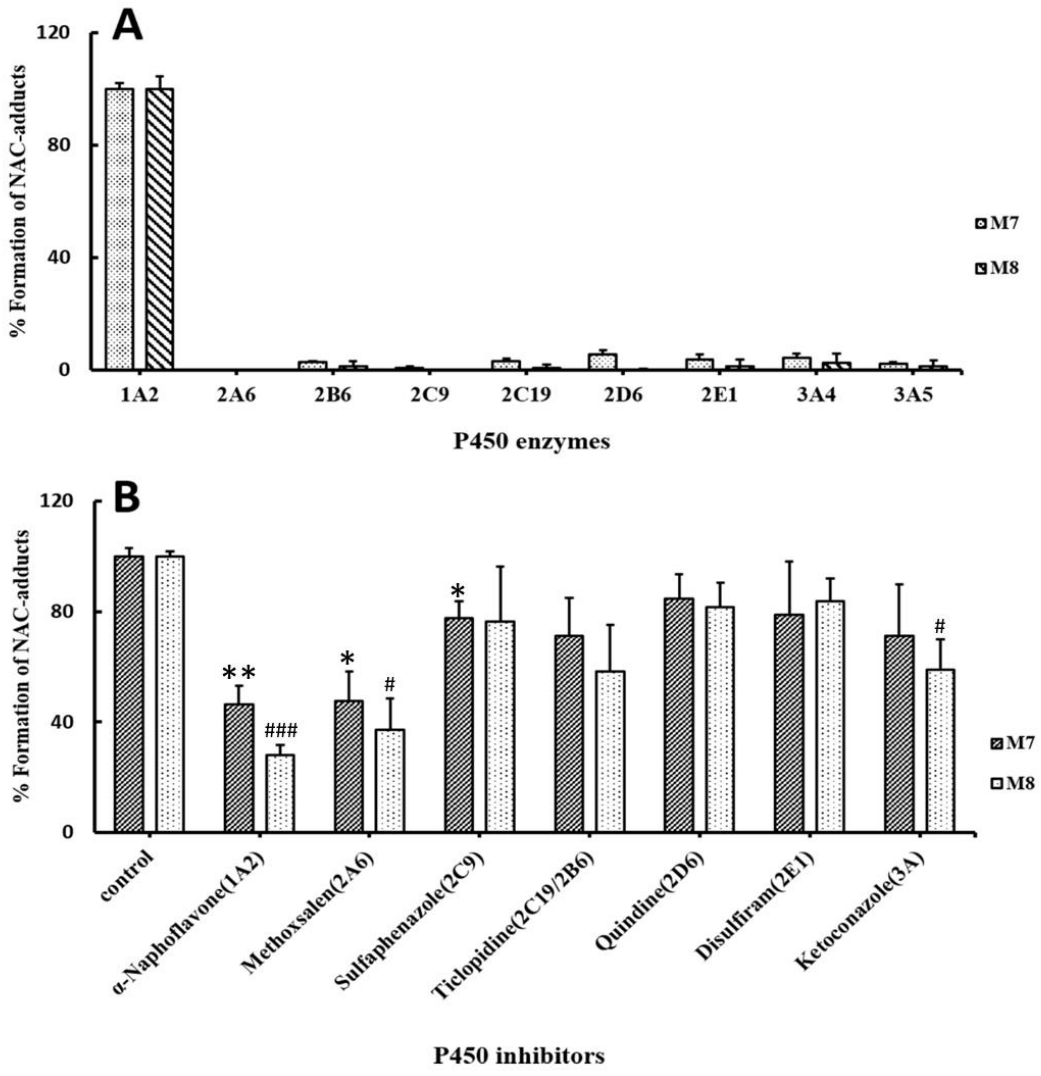
A
120
80
40
0
% Formation of NAC-adducts
M7
M8
1A2
2A6
2B6
2C9
2C19
2D6
2E1
3A4
3A5
P450 enzymes
B
120
80
40
0
% Formation of NAC-adducts
**
###
*
#
*
#
M7
M8
control
α-Naphoflavone(1A2)
Methoxsalen(2A6)
Sulfaphenazole(2C9)
Ticlopidine(2C19/2B6)
Quindine(2D6)
Disulfiram(2E1)
Ketoconazole(3A)
P450 inhibitors

Figure 11

Table 1. Effects of $K_3Fe(CN)_6$ on the inactivation of CYP3A.

System	CYP3A	
	% Control (0 min)	% Control (20 min)
-KFC	**50.7±2.9**	**40.5±2.6**
+KFC	**86.3±8.4**	**80.2±15.7**
% Reversed	**/**	**39.7**

KFC, potassium ferricyanide. Data represent the mean±SD (n=3). The percentage of CYP3A activity was determined by calculation of the ratio of enzyme activity of each sample after 0 or 20 min incubation with PPR vs. that of the corresponding control sample without PPR treatment. % Reversed stands for the contribution of KFC to the recovered activity of CYP3A.